CHINESE JOURNAL OF PHYSICS VOL. 53, NO. 2 April 2015

Elastic and Mechanical Properties of Cubic Diamond under Pressure

E. Güler* and M. Güler

Hitit University, Department of Physics, 19030 Corum, Turkey
(Received September 30, 2014; Revised December 20, 2014)

We report on some structural, elastic, and mechanical properties of cubic diamond under pressures up to 500 GPa. Unlike existing theoretical works, the second-generation reactive bond order (REBO) potential was used for the first time to elaborate the *pressure dependence* properties of cubic diamond through geometry optimization calculations. The pressure dependence of the density, typical cubic elastic constants, bulk, shear, and Young moduli, Poisson ratio, elastic velocities, anisotropy parameter, Kleinman parameter, and stability conditions of diamond were evaluated. Our results are in reasonable agreement with the experimental findings and published theoretical data.

DOI: 10.6122/CJP.20141230 PACS numbers: 62.20.D-, 62.50.-p, 81.05.ug

I. INTRODUCTION

The elastic properties of materials under pressure provide better understanding of some basic physical aspects such as interatomic forces, elasticity, mechanical features, phase transitions and so forth. Nonetheless, elastic property measurements under pressure are usually challenging, and the lack of experimental data can be compensated by computational methods [1, 2].

Diamond has remarkable physical features, since it has high thermal conductivity, low thermal expansion, high optical transparency, ultra hardness, and good insulating capacity. Therefore, diamond is one of the key materials for today's technology, since it covers a wide range of uses, ranging from high pressure Anvil Cell experiments to several medical applications [3–6].

Apart from the limited high pressure experiments [7–9], there are many theoretical investigations linking with the various physical properties of diamond. In 1999, Xie *et al.* [10] analysed the thermal expansion, bulk modulus, and phonon structure of diamond with the quasiharmonic approximation within density functional theory (DFT). Later, Blumenau and colleagues [11] determined the bulk modulus and elastic constants of diamond with the density functional based tight binding (DFTB) method in 2002. Wang and Ye also calculated the elastic properties of diamond in 2003 by using the plane wave pseudo potential (PWPP) method [12]. Monet and Marzari stated the structural, dynamical, and thermodynamic properties of diamond with the generalized gradient approximation (GGA) via DFT in 2005 [13]. Afterwards, Gao and co-workers applied the second-generation REBO

*Electronic address: eguler71@gmail.com

potential to molecular dynamics (MD) calculations in 2006 to obtain the *temperature dependence of* the elastic parameters of diamond [14]. Fu *et al.* conducted DFT calculations by applying three exchange-correlation Hamiltonian functionals as restricted close shell Hartree-Fock functions (RHF), unrestricted open shell Hartree-Fock functions (UHF), and the B3PW form of DFT [3] in 2009. Subsequently, Valdez, Umemoto, and Wentzcovitch used the local density approximation (LDA) with the DFT in 2012 for the high pressure and high temperature elasticity of diamond [15]. In this work, unlike the above theoretical calculations, we report on the application of the second-generation REBO potential for the first time to assess the *pressure dependence* of the density, typical cubic elastic constants, bulk, shear, and Young moduli, Poisson ratio, elastic velocities, anisotropy parameter, Kleinman parameter, and stability conditions of diamond.

The rest of the paper is organized as follows. After this introduction, a brief outline for the geometry optimization and computational details are given in Section II. Our calculation results are given and discussed in Section III. We then summarize and conclude in Section IV.

II. COMPUTATIONAL DETAILS

Geometry optimization is a reliable method for both the MD and DFT methods to get a stable configuration for a molecule or periodic system through efficient and inexpensive energy computations. An optimization procedure involves the repeated sampling of the potential energy surface until the potential energy reaches a minimum where all forces on all atoms are zero. All herein done geometry optimization calculations were performed with the General Utility Lattice Program (GULP) MD code 4.0. [16, 17]. This code allows wide-range property calculations for 3D periodic solids, 2D surfaces, and gas phase clusters by employing two-body, three-body, four-body, six-body, and many body (EAM) potentials [1, 18, 19] depending on the demands of the research. Since REBO potentials provide satisfactory results for carbon and related structures, we employed a second-generation REBO potential [20] for our diamond research. To make a quantitative comparison with the B3PW results [3], the lattice constant for cubic diamonds was set to the same value as Ref. [3], 3.5707 Å, which is slightly higher than the experimental lattice constant = 3.5606 Å and with the space group Fdm (OH7). Details of the applied second-generation REBO type potential and its procedure can be also found in Ref. [20].

It is possible to optimize the related structures at constant pressure (includes all internal and cell variables) and constant volume (unit cell remains frozen) with the GULP MD code [1, 2, 16, 17]. Constant pressure optimization was chosen for diamond in the present study. The geometry of the cells was optimized by the Newton–Raphson method based on the Hessian matrix calculated from the second derivatives. The Hessian matrix was also recursively updated during optimization by using the BFGS [1, 2, 16, 17] algorithm. After setting the preconditions for the cubic crystal structure of diamond, we adopted multiple runs at zero Kelvin temperature and checked the pressure ranges starting from 0 GPa up to 500 GPa.

III. RESULTS AND DISCUSSION

Fig. 1 shows the pressure dependence of density in diamond. As in many materials, the density of diamond shows a smooth increment with increasing pressure. As well, Fig. 2. outlines a comparison for the typical cubic elastic constants of diamond between our results (circles) and former B3PW-DFT data (squares) [3]. The three typical and independent elastic constants (C_{11}, C_{12}, and C_{44}) define the mechanical hardness and are necessary for specifying the stability of the material. These constants are usually derived from the total energy calculations representing the single crystal elastic properties. At this point, the Voigt-Reuss-Hill approach is a confident scheme for the elastic constants of polycrystalline materials [2]. To capture the correct values of the elastic constants and relevant parameters of diamond, we considered the Voigt-Reuss-Hill values during calculations. Further, cubic elastic constants show a straight increment with pressure in the entire pressure range as in Fig. 2. Besides, the increment of C_{11} is higher than that of both C_{12} and C_{44}. In a physical sense, C_{11} stands for the longitudinal elastic behavior, whereas C_{12} and C_{44} explain the off diagonal and elastic shear characteristic of cubic crystals, respectively. So, a longitudinal strain produces a change in volume without a change in shape. This volume change is related to pressure, and thus reflects a larger change in C_{11}. In contrast, a transverse strain or shearing causes a change in shape without a change in volume. So, C_{12} and C_{44} are less sensitive to pressure than C_{11}. Our results for the cubic elastic constants are consistent with the experiments and show some similarity with the earlier DFT data [3]. Beyond Fig. 2., Table I lists numerical values of the cubic elastic constants with the available experimental and theoretical data for the sake of comparison.

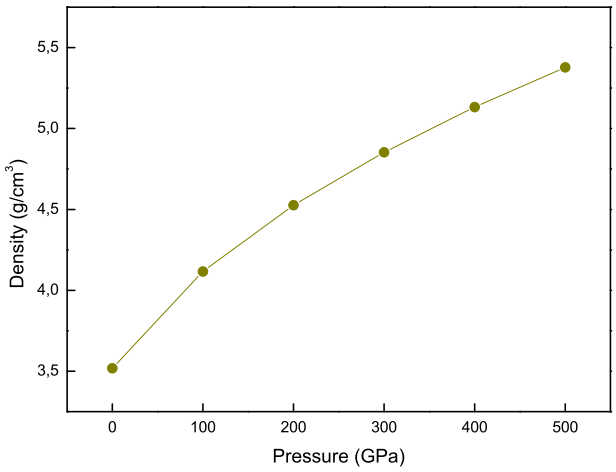

FIG. 1: Density of diamond under pressures up to 500 GPa.

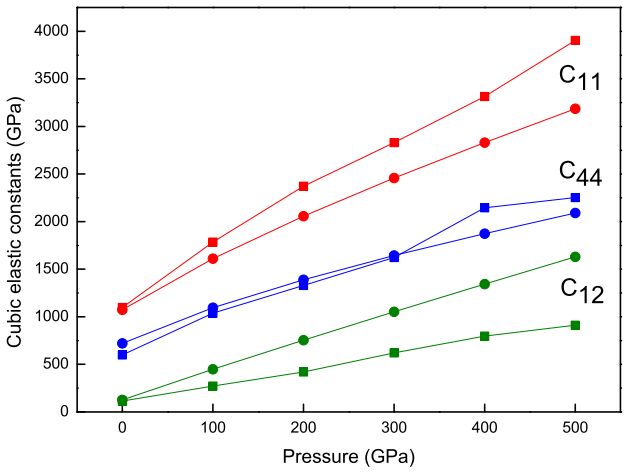

FIG. 2: Comparing the typical cubic elastic constants of diamond under pressure. The squares denote the former DFT data [Ref. 3] whereas the circles display our data.

According to Born structural stability, the elastic constants must satisfy the conditions $C_{11} - C_{12} > 0$, $C_{11} > 0$, $C_{11} + 2C_{12} > 0$, and cubic stability, for example: $C_{12} < B < C_{11}$ [1, 2]. As another result, the present C_{11}, C_{12}, and C_{44} values well confirm both the structural and cubic stability conditions for diamond. From an extra structural outlook, the cohesive energy (E_{coh}) is an essential physical quantity that accounts for the strength of the bonds in a material and can be determined experimentally or computed using theoretical methods [19]. It is very clear that our calculation results indicate a perfect correspondence with the prior experimental results of diamond (see Table I).

The bulk modulus (B) yields much information about the bonding strength of materials, and it is a measure of resistance to external deformation [1, 2, 19, 21]. Fig. 3 displays a further comparison for the pressure behavior of the bulk modulus in diamond for the considered pressure scale. The closed circle symbols denote our results and the squares show the B3PW-DFT findings of Ref. [3]. From the common physical equation of the bulk modulus ($B = \Delta P/\Delta V$), one can expect an increment for B, because of its direct proportion to applied pressure. Thus, the bulk modulus of diamond dramatically increases in Fig. 3 for both the present and former data under pressure. By the way, the shear modulus, (G) describes the resistance to shape change caused by a shearing force [1, 2, 21]. The Young modulus (E) is the resistance to uniaxial tensions and gives the stiffness degree, i.e., the higher the value of E, the stiffer is the material [1, 2, 21]. Like the bulk modulus, the shear and Young moduli of diamond also point out the same behavior under pressure as in Fig. 4.

Since ductility and brittleness play a critical role during the production of materials, we also appraised the ductile (brittle) nature of diamond under pressure. The adjectives brittle and ductile signify two different mechanical behaviors of solids when they are sub-

TABLE I: Comparing some structural, elastic, and mechanical parameters of diamond with the previous and present results.

Parameter	Present	Experiments	Other theoretical	
	REBO		B3PW[3]	LDA
a (Å)	3.57	3.56[31]	3.57	3.53[32]
d (g/cm^3)	3.51	3.52[32]		3.60[32]
E_{coh} (eV/atom)	7.36	7.37[32]		8.67[32]
C_{11} (GPa)	1074.8	1079[33]	1097.5	1078.9[15]
C_{12} (GPa)	125.6	124[33]	115.5	140.8[15]
C_{44} (GPa)	720.6	578[33]	598.2	577.3[15]
B (GPa)	442	442[33]	442.8	453.5[15]
G (GPa)	609.5	535[33]	552.7	531.3[15]
E (GPa)	1048.5			
ν	0.1	0.1[34]		
V_L (km/s)	18.8			
V_S (km/s)	13.1			
ζ	0.26		0.25	
A	1.51		1.21	

jected to stress. In general, brittle materials are not deformable or less deformable before fracture. Unlike brittle materials, ductile materials are deformable a lot before fracture. At this point, the Pugh ratio is a determinative limit for ductile (brittle) behavior and has a popular use in the literature. If the G/B ratio is about 0.571 and higher, the material is brittle, otherwise the material becomes ductile.

The Pettifors Cauchy pressure is an alternative evaluation criterion for ductility and brittleness, which is formulated as $C_P = C_{12} - C_{44}$ [2]. The negative (positive) values of the Pettifors Cauchy pressure show the brittle (ductile) nature of compounds. Niu *et al.* [22] combined these two criteria (Pugh and Pettifor) for a universal ductile-brittle criterion and also normalized $C_{12} - C_{44}$ values by the young modulus (E) which resulted in a nice parabola including cubic diamond. So, we checked the present results through the scheme of Niu *et al.* [22]. Fig. 5 is a combined plot of $(C_{12} - C_{44})/E$ vs. the (G/B) ratio of diamond up to 500 GPa. As in their findings [22], cubic diamond appears in the lower right corner due to the presence of directional covalent bonding, resulting in a brittle behavior. Our value at 0 GPa is obtained to be 1.37 and compares well with the DFT value of 1.2 of Niu *et al.* [22]. After a careful look, it is easy to see that our renormalized values always appear in the lower right corner up to 500 GPa, in which all results sustain the brittle nature of

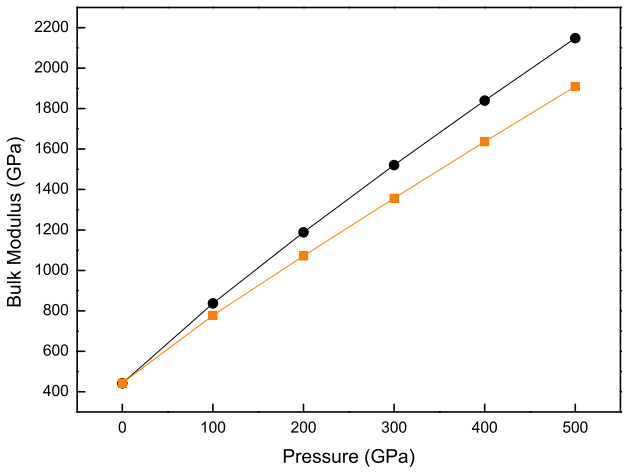

FIG. 3: Pressure dependence of bulk modulus in diamond. Again, squares denote the former DFT data [Ref. 3] whereas circles represent our data.

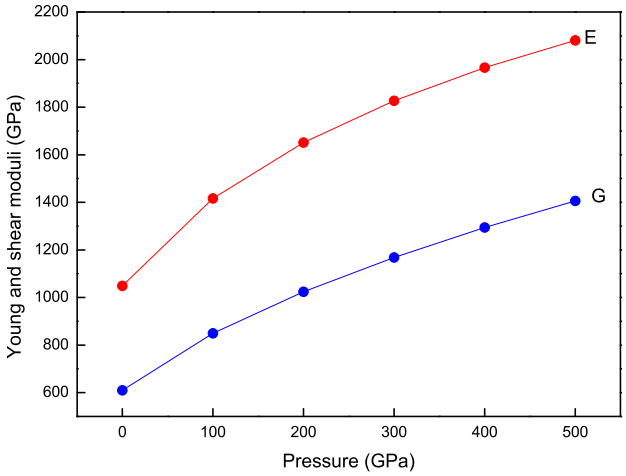

FIG. 4: Pressure dependence of E and G moduli in diamond.

diamond.

The Poisson ratio (ν) is the ratio between the transverse strain (e_t) and longitudinal strain (e_l) in the elastic loading direction [2, 19, 23]. It delivers detailed knowledge about the bonding character of solids. In general, the Poisson ratio values are of about 0.1 for covalent

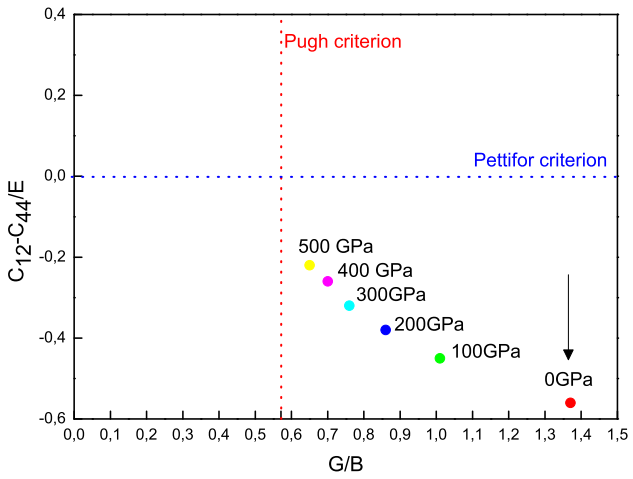

FIG. 5: Renormalized Pugh and Pettifor critera for cubic diamond under various pressures.

materials, 0.25 for ionic materials and change between 0.28 and 0.42 for metals [1, 2, 19, 23–30]. As in Fig. 6, the Poisson ratio of diamond at 0 GPa is 0.1, which reflects the covalent bonding nature of diamond and is consistent with the experiments. (See Table I). So as a combined result, the relatively low values of B/G hence ν for diamond dictates the high degree of covalent bonding for cubic diamond.

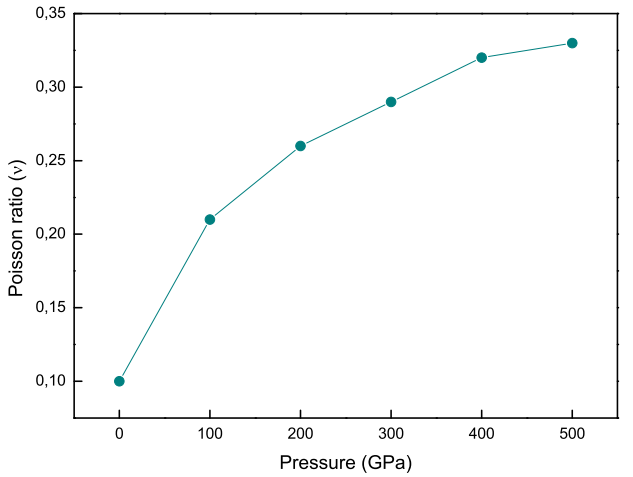

FIG. 6: Poisson ratio behavior under pressure for diamond.

In solids,the low-temperature acoustic modes trigger the vibrational excitations. Being dependent on this case, two typical elastic waves, namely the longitudinal wave and shear wave arise [1, 2, 19, 23]. V_L and V_S refer to the velocities of these waves, respectively, Fig. 7 depicts these velocities along the [100] direction of cubic diamond under pressure. Both V_L and V_S of diamond has an increment trend with the increasing pressure as in Fig. 7.

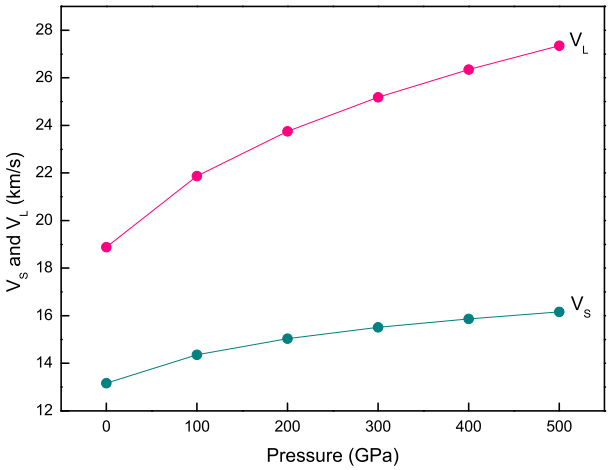

FIG. 7: Pressure dependence of elastic wave velocities of (V_L and V_S) in diamond up to 500 GPa.

The Kleinman parameter (ζ) for cubic materials describes the relative ease of bond bending to the bond stretching. Minimizing bond bending leads to $\zeta = 0$ and minimizing bond stretching leads to $\zeta = 1$. In addition, the Kleinman parameter links to the elastic constants as $\zeta = C_{11} + 8C_{12}/7C_{11} + 2C_{12}$ [2, 23]. Fig. 8 displays the Kleinman parameter of diamond upon pressure increment. Under pressure, ζ increases with increasing pressure and it is found to be between 0.26 and 0.64.

The elastic anisotropy of crystals is important for engineering since it is correlated with the possibility of producing microcracks in materials. For that reason, the anisotropy factor $A = 2C_{44}/(C_{11} - C_{12})$ [2, 23] has been evaluated for a deeper view on the elastic anisotropy of diamond. For an ideal isotropic system (A) is unity and a deviation from unity gives the amount of elastic anisotropy. Fig. 9 show the anisotropy behavior of cubic diamond. As in Fig. 9, the calculated anisotropy factors (A) are between 1.51 and 2.68 for the applied pressure range, which indicates the significant presence of elastic anisotropy in diamond.

In summary, the results of the current study show a fair agreement with the experiments, especially on the density, cohesive energy, and bulk modulus of cubic diamond, as is clear in Table I. Also, typical cubic elastic constants agree with both the experiments and prior theoretical data. Although the value of the shear modulus slightly overestimates

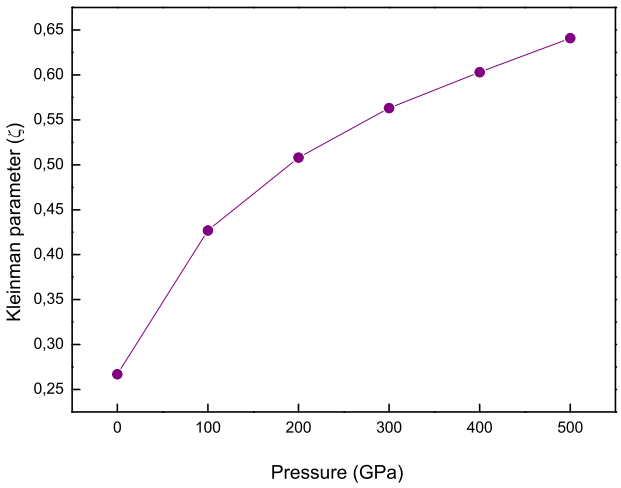

FIG. 8: Behavior of the Kleinman parameter under pressure for diamond.

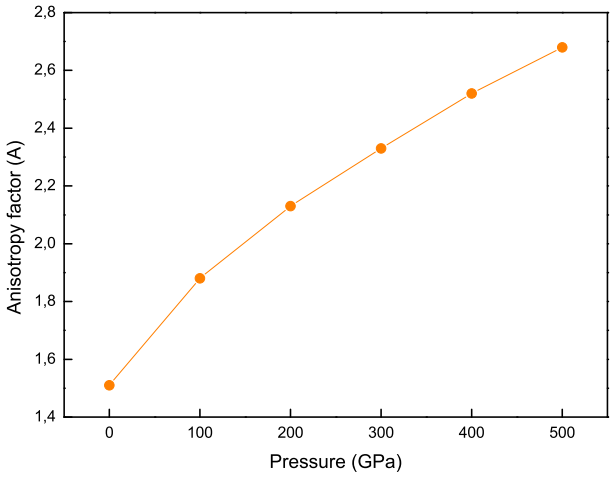

FIG. 9: Anisotropy factor of diamond versus pressure.

the measurements, it does not alter the brittle character of cubic diamond. On the other hand, the obtained Poisson ratio value corroborates the well-known covalent bonding nature of diamond and gives credence to the present work. Overall, our results agree well with both the experiments and earlier DFT calculations [3, 15, 31–34] (See Table I). The negligible deviations between our results and the earlier theoretical data seem to be due to

the difference between the methodologies used in the calculations.

IV. CONCLUSIONS

It should be noted that this work reports the use of a different and effective method by applying a proper potential and addresses the pressure dependence of the density, bulk modulus, shear modulus, Young modulus, Poisson ratio, elastic wave velocities, Kleinman parameter, and anisotropy of cubic diamond up to 500 GPa. The use of a second-generation REBO potential through geometry optimization calculations well reproduce the mechanical, structural, and elastic data of diamond under pressure. Finally, our detailed results are about experiments and can be used for the lack of experimental data. The present findings may also contribute to future theoretical works of diamond under pressure.

References

[1] E. Güler and M. Güler, Adv. Mater. Sci. Eng. **2013**, Article ID 525673 (2013).
[2] E. Güler and M. Güler, Mater. Res. Ibero. Am. J. **17**, 1268 (2014).
[3] Z. J. Fu *et al.*, Commun. Theor. Phys. **51**, 1129 (2009). doi: 10.1088/0253-6102/51/6/31
[4] Q. Huang *et al.*, Nature **510**, 250-253 (2014). doi: 10.1038/nature13381
[5] R. J. Narayan *et al.*, Materials Today **14**, 154 (2011). doi: 10.1016/S1369-7021(11)70087-6
[6] S. Ono, K. Mibe, and Y. Ohishi, J. Appl. Phys. **116**, 053517 (2014). doi: 10.1063/1.4891681
[7] F. Ocelli, P. Loubeyre, and R. Letoullec, Nat. Mater. **2**, 151 (2003).
[8] I. V. Aleksandrov *et al.*, High Press. Res. **1**, 333 (1989). doi: 10.1080/08957958908202491
[9] Ph. Gillet *et al.*, Phys. Rev. B **60**, 14660 (1999). doi: 10.1103/PhysRevB.60.14660
[10] J. J. Xie *et al.*, Phys. Rev. B **60**, 9444 (1999). doi: 10.1103/PhysRevB.60.9444
[11] A. T. Blumenau *et al.*, Phys. Rev. B **65**, 205205 (2002). doi: 10.1103/PhysRevB.65.205205
[12] S. Q. Wang and H. Q. Ye, J. Phys. Condens. Matter. **15**, 5307 (2003). doi: 10.1088/0953-8984/15/30/312
[13] N. Mounet and N. Marzari, Phys. Rev. B **71**, 205214 (2005). doi: 10.1103/PhysRevB.71.205214
[14] G. Gao *et al.* ,J. Phys.: Condens. Matter. **18**, S1737 (2006). doi: 10.1088/0953-8984/18/32/S05
[15] M. N.Valdez, K. Umemoto, and R. M. Wentzcovitch, Appl. Phys. Lett. **101**, 171902 (2012). doi: 10.1063/1.4754548
[16] J. D. Gale and J. Chem. Soc. Faraday **93**, 629 (1997). doi: 10.1039/a606455h
[17] J. D. Gale and A. L. Rohl, Mol. Simulat. **29**, 291 (2003). doi: 10.1080/0892702031000104887
[18] J. D. Gale and Z. Kristallogr, **220**, 552 (2005). doi: 10.1524/zkri.220.5.552.65070
[19] M. Güler and E. Güler, Chin. Phys. Lett. **30**, 056201 (2013). doi: 10.1088/0256-307X/30/5/056201
[20] D. W. Brenner *et al.*, J. Phys.: Condens. Matter **14**, 783 (2002). doi: 10.1088/0953-8984/14/4/312
[21] S. Bensalem *et al.*, J. Alloy. Compd. **589**, 137 (2014). doi: 10.1016/j.jallcom.2013.11.113
[22] H. Niu *et al.*, Sci. Rep. **2**, 1 (2012). doi: 10.1038/srep00718
[23] E. Güler and M. Güler, Chin. J. Phys. **52**, 1625 (2014).
[24] O. Boudrifa *et al.*, J. Alloy. Compd. **618**, 84 (2015). doi: 10.1016/j.jallcom.2014.08.143
[25] M. Ameri *et al.*, Materials Science in Semiconductor Processing **16**, 1508 (2013). doi:

10.1016/j.mssp.2013.05.003
[26] D. Varshney, S. Shriya, and R. Khenata, Mater. Chem. Phys. **135**, 365 (2012). doi: 10.1016/j.matchemphys.2012.04.060
[27] D. Varshney *et al.*, Eur. Phys. J. B **79**, 495 (2011). doi: 10.1140/epjb/e2011-10641-1
[28] D. C. Gupta and K. C. Singh, Sol. Stat. Sci. **12**, 1809 (2010). doi: 10.1016/j.solidstatesciences.2010.07.036
[29] D. C. Gupta and G. S. Raypuria, Eur. Phys. J. B **84**, 99 (2011). doi: 10.1140/epjb/e2011-10857-y
[30] M. Güler and E. Güler, J. Optoelectron. Adv. Mater. **16**, 12222 (2014).
[31] T. Sato *et al.*, Phys. Rev. B **65**, 092102 (2002). doi: 10.1103/PhysRevB.65.092102
[32] H. J. Cui *et al.*, arXiv:1310.5228v1 [cond-mat.mtrl-sci] 19 Oct 2013.
[33] H. J. McSkimin and P. Andreatch, Jr. J. Appl. Phys. **43**, 2944 (1972). doi: 10.1063/1.1661636
[34] K. J. Gray, Proc. SPIE, Diamond Optics V **1759**, 203 (1992). doi: 10.1117/12.130773